

1 **Annual evapotranspiration retrieved from satellite**
2 **vegetation indices for the Eastern Mediterranean at 250 m**
3 **spatial resolution**

4
5 **D. Helman¹, A. Givati² and I. M. Lensky¹**

6 [1]{Department of Geography and Environment, Bar Ilan University, Ramat-Gan, Israel}

7 [2]{Israeli Hydrological Service, Water Authority, Jerusalem, Israel}

8
9 Correspondence to: D. Helman (davidhelman.biu@gmail.com)

10

11 **Abstract**

12 We present a simple model to retrieve actual evapotranspiration (ET) from satellites'
13 vegetation indices (PaVI-E) for the Eastern Mediterranean (EM) at a spatial resolution of 250
14 m. The model is based on the empirical relationship between satellites' vegetation indices
15 (NDVI and EVI from MODIS) and total annual ET (ET_{Annual}) estimated at 16 FLUXNET sites
16 representing a wide range of plant functional types and ET_{Annual} . Empirical relationships were
17 first examined separately for (a) annual vegetation systems (i.e., croplands and grasslands)
18 and (b) systems with combined annual and perennial vegetation (i.e., woodlands, forests,
19 savannah and shrublands). Vegetation indices explained most of the variance in ET_{Annual} in
20 those systems (71% for annuals, and 88% for combined annuals and perennials systems)
21 while adding land surface temperature data in multiple regression and modified Temperature
22 and Greenness models did not result in better correlations ($p>0.1$). After establishing
23 empirical relationships, PaVI-E was used to retrieve ET_{Annual} for the EM from 2000 to 2014.
24 Models' estimates were highly correlated ($R = 0.92$, $p<0.01$) with ET_{Annual} calculated from
25 water catchment balances along rainfall gradient of the EM. They were also comparable to the
26 coarser resolution ET products of MSG (LSA-SAF MSG ETa, 3.1 km) and MODIS (MOD16,
27 1 km) at 148 EM basins with R of 0.75 and 0.77 and relative biases of 5.2 and -5.2%,
28 respectively ($p<0.001$ for both). In the lack of high-resolution (<1 km) ET models for the EM

1 the proposed model is expected to contribute to the hydrological study of this region assisting
2 in water resource management, which is one of the most valuable resources of this region.

4 **1 Introduction**

5 Actual evapotranspiration (ET) is a primary component of the global water cycle. Its
6 assessment at global and regional scales is essential for forecasting future atmospheric
7 feedback (Jung et al., 2010; Oki and Kanae, 2006; Zemp et al., 2014). Estimating ET at such
8 scales though, is not straightforward and requires the use of models (Chen et al., 2014; Hu et
9 al., 2015; Jung et al., 2009; Trambauer et al., 2014). Data-driven models using satellite
10 information benefit from a continuous spatio-temporal direct observation of the land surface
11 (Ma et al., 2014; Shi and Liang, 2014).

12 Satellite-based ET models are classified into two: (1) empirical, using the relationship
13 between in situ ET and satellites-derived vegetation indices (VIs) (Glenn et al., 2011; Nagler
14 et al., 2012; Tillman et al., 2012) and (2) physical, using surface temperature from satellites to
15 solve energy balance equations (Anderson et al., 2008; Colaizzi et al., 2012). While some
16 models combine the two approaches (Tsarouchi et al., 2014).

17 Although physical-based models are much more common their performance is comparable to
18 that of the empirical-based models (Glenn et al., 2010). The accuracy of both approaches is
19 within that of the eddy covariance measurements (70-90%) used for their calibration or
20 validation (Kalma et al., 2008). Yet, the empirical approach is simpler than the physical-based
21 model and requires less additional information.

22 The basis for the empirical model is the resource optimisation theory. This theory suggests
23 that plants adjust their foliage density to the environmental capacity to support photosynthetic
24 activity and transpiration (Glenn et al., 2010). Accordingly, changes in vegetation foliage
25 cover (and VIs) would affect ET resulting in high ET-VIs correlations. Then, the empirical
26 equation could be used to retrieve ET in space and time.

27 This approach is mostly used in vegetation systems with annual cycle of growth and drying
28 where VIs define well the phenological stages (Glenn et al., 2011; Senay et al., 2011).
29 However, in complex systems comprised of annual (i.e., herbaceous) and perennial (i.e.,
30 woody) vegetation the model must be adjusted with additional meteorological data (Maselli et
31 al., 2014).

1 The main drawback of the empirical-based approach is that it is limited to a specific site and
2 vegetation type (Glenn et al., 2010; Maselli et al., 2014; Nagler et al., 2012). No common
3 relationship was found between ET and VIs for different sites and climatic conditions.

4 Here we used MODIS VIs and land surface temperature (LST) products and eddy covariance
5 ET from 16 FLUXNET sites with different plant functional types to establish empirical
6 relationships between VIs (and/or LST) and ET in Mediterranean vegetation systems. We first
7 examined those relationships in annual vegetation systems and complex systems comprising
8 both annuals and perennials vegetation. Three empirical models were examined: (1) simple
9 regression, (2) multiple variable and (3) modified Temperature and Greenness models with
10 16-day and mean annual data. We used a performance-simplicity criterion to choose the best
11 model to retrieve ET for the EM. Estimates were compared with MODIS and MSG ET
12 operational products and evaluated against ET calculated from water catchment balances in
13 the EM.

14 15 **2 Data**

16 **2.1 Evapotranspiration from eddy covariance towers**

17 In situ ET was derived from eddy covariance towers that constitute the international flux
18 towers net (FLUXNET). Two open FLUXNET sources were used to acquire the datasets: the
19 Oak Ridge National Laboratory Distributed Active Archive Centre (available online
20 [<http://fluxnet.ornl.gov>] from ORNL DAAC, Oak Ridge, Tennessee, U.S.A) and the
21 European fluxes database [<http://gaia.agraria.unitus.it/home>]. Half-hourly level 4 ET data
22 were checked for acceptable quality (Reichstein et al., 2005) and gap-filled using methods
23 described in Reichstein et al. (2005) and Moffat et al. (2007). Then, data were aggregated to
24 16-day means (mm d^{-1}) and total annual ET (mm yr^{-1}). Only ET data since the time MODIS
25 VIs products are available were used (i.e., since 2000).

26 **2.2 Satellite products**

27 We used 16-day NDVI and EVI at a spatial resolution of 250 m (MOD13Q1) and 8-day LST
28 at 1 km spatial resolution (MOD11A2) from MODIS on board Terra satellite. Although Terra
29 provides LST twice a day (around 10:30 a.m./p.m. local time) here we used only daytime
30 LST, which is the relevant for ET processes. The 8-day LST were averaged to match the 16-

1 day temporal resolution of the VIs product.

2 The MODIS 16-day VIs product is a composite of a single day value selected from 16 days
3 period based on a maximum value criterion (Huete et al., 2002). It represents the vegetation
4 status of the entire 16-day period because of the gradual development of the vegetation. This
5 enables regressing MODIS VIs product against 16-day averages of ET. NDVI is defined as
6 (Rouse et al., 1974):

$$7 \quad NDVI = \frac{R_{0.8} - R_{0.6}}{R_{0.8} + R_{0.6}} \quad (1)$$

8 and EVI as (Huete et al., 2002):

$$9 \quad EVI = 2.5 \times \frac{R_{0.8} - R_{0.6}}{R_{0.8} + 6R_{0.6} - 7.5R_{0.5} + 1} \quad (2)$$

10 where $R_{0.8}$, $R_{0.6}$ and $R_{0.5}$ are the reflectance at near infrared (0.8 μm), red (0.6 μm) and blue
11 (0.5 μm) bands, respectively. NDVI suffers from asymptotic problems (saturation) over high
12 density of vegetation biomass while EVI is more sensitive in such cases (Huete et al., 2002).

13 For model development, time series of NDVI, EVI and LST at each FLUXNET site were
14 obtained from MODIS Land Product Subsets [<http://daac.ornl.gov/MODIS/modis.html>]
15 (ORNL DAAC, Oak Ridge, Tennessee, U.S.A., last accessed December 2014) for the years
16 when ET data was available since 2000 (see ‘Period’ column in Table 1). NDVI and EVI time
17 series were smoothed using local weighted scatterplot technique (LOWESS) as in Helman et
18 al. (2014a, 2014b and 2015). For model implementation, tiles h20v05, h21v05, h20v06 and
19 h21v06 of the MOD13Q1 product were downloaded for 2000–2014 using the USGS
20 EarthExplorer tool [<http://earthexplorer.usgs.gov>]. These tiles fully cover the Eastern
21 Mediterranean region.

22 Model results were compared with two satellite operational ET products from MODIS
23 (MOD16) and MSG (LSA-SAF MSG ETa) in 2011 at 148 main basins in the Eastern
24 Mediterranean. MODIS and MSG ET products are based on different physical models, and
25 have different spatial and temporal resolutions (1km/8day for MODIS, and 3.1km/daily for
26 MSG) (Hu et al., 2015). The annual MODIS (MOD16A3) and daily MSG (LSA-SAF MSG
27 ETa) ET products were downloaded for 2011 for the EM region. The basins map was taken
28 from HydroSHEDS, a mapping product based on high-resolution elevation layer developed
29 by the Conservation Science Program of World Wildlife Fund

1 (<http://hydrosheds.cr.usgs.gov>). Only main basins with an area greater than 10 km² were
2 selected (Fig. S1).

3 **2.3 Evapotranspiration from water catchment balances for validation**

4 We evaluated our model with mean annual ET calculated from six water catchment balances
5 along a north-south rainfall gradient (130 – 800 mm yr⁻¹) in the Eastern Mediterranean (Fig.
6 S2 and Table 2). The calculation follows the classical water balance equation:

$$7 \quad ET = P - Q - \frac{dS}{dt} \quad (3)$$

8 where P and Q are the total annual precipitation and discharge measured in the catchment,
9 and dS/dt is the change in water storage.

10 Precipitation data (P) were collected for 2000-2013 from a total of 30 stations of the Israel
11 Meteorological Service: 5 in Kziv, 2 in HaShofet, 21 in the Mountain Aquifer (north, centre
12 and south) and 2 stations in the Mamashit catchment. Data were interpolated for the entire
13 catchment area using ArcGIS and the inverse-distance weighting (IDW) methodology (Lu
14 and Wong, 2008). Discharges (Q) were measured for the same period (2000-2013) for Kziv,
15 Hashofet and Mamashit catchments using runoff gauges of the Hydrological Service of Israel
16 (HSI) in: Gesher Haziv hydrometric station for Kziv, HaShofet-Hazorea for HaShofet and
17 Mamashit station for the Mamashit catchment. Annual runoffs at the upper parts of the
18 Mountain Aquifer (drainage areas without hydrometric stations at the Hedera, Alexander,
19 Yarkon, Ayalon, Soreq and Lachish basins) were calculated using the HEC-HMS (Hydrologic
20 Engineering Centre – Hydrologic Modelling System) model (Feldman, 2000) run by the HSI
21 (<http://www.water.gov.il>).

22 For timescales of several years dS/dt is assumed to be negligible ($dS/dt = 0$) so the mean
23 annual ET could be simply calculated from P minus Q (Conradt et al., 2013). Following this
24 assumption, we averaged water components over the 14 years of data (i.e., 2000-2013) to
25 calculate mean annual ET. Water balances components (P and Q) and calculated mean annual
26 ET for the six catchments are presented in Table 2.

27 Calculating ET from water balances has some drawbacks like the difficulty to properly
28 estimate the spatial distribution of precipitation over the entire catchment and uncertainties of
29 catchment boundaries (Conradt et al., 2013). However, this is the best existing approach to
30 compare in situ ET with satellite-derived ET at a basin scale.

1

2 **3 Methods**

3 **3.1 Site selection**

4 Perennial and annual vegetation in Mediterranean regions have distinct phenology
5 contributing differently to the VIs signal (Helman et al., 2015; Karnieli, 2003; Lu et al.,
6 2003). Here we examined VIs - ET relationships in vegetation systems comprising both
7 annual and perennial vegetation (i.e., forests, woodlands, savannah and shrublands, hereafter
8 PA) separately from those comprising only annual vegetation (i.e., croplands and grasslands,
9 hereafter AN).

10 We found that annual vegetation in the understory of PA systems might contribute
11 significantly to VIs while having very small contribution to the total ecosystem ET. In some
12 cases, this results in an apparent phase shift between ET and VIs (Fig. 1) leading to negative
13 or a lack of correlation. Moreover, we found that AN sites exhibit one single ET–VI
14 relationship under wide range of rainfall conditions whereas similar types of PA systems have
15 significantly different ET – VI relationships (i.e., different slopes) under different climatic
16 regimes (Unpublished results).

17 Therefore, AN sites (FLUXNET sites in AN systems) were selected from wide range of
18 climatic regimes while PA sites (FLUXNET sites in PA systems) were selected only from
19 Mediterranean-climate regions. Selection of the FLUXNET sites had to fulfil the following
20 criteria: (1) at least three years of satellite and eddy covariance data in the FLUXNET site; (2)
21 missing data less than 30 days yr⁻¹ for ET and 15% for VIs; and (3) homogeneous vegetation
22 cover near the FLUXNET tower within at least the 250 m spatial resolution of the MODIS
23 VIs product. The last criterion was manually assured using Google EarthTM. These led us to
24 select 16 FLUXNET sites that represent a wide range of plant functional types and ET rates
25 (Table 1, Figures S3 and S4).

26 **3.2 Empirical ET models using VIs and LST**

27 Three regression models were examined using the satellite-derived NDVI, EVI, LST and
28 eddy covariance ET data:

29 (1) Simple regressions of ET against VIs or LST with 16-day and annual data.

1 (2) Multiple variable regressions using NDVI (or EVI) and LST as dependent variables
2 and ET as the independent variable. Regressions were conducted with both, 16-day
3 averages and annual data

4 (3) Modified version of the Temperature and Greenness (TG) model proposed by Sims et
5 al. (2008) using LST as a proxy for radiation and potential ET (Maeda et al., 2011)
6 with 16-day data alone.

7 We used all models with 16-day ET averages and 16-day VIs and/or LST data but only the
8 first two models with total annual ET and mean annual VIs and/or LST because the TG model
9 was designed to work only with 16-day data (Sims et al. 2008). In AN, we subtracted the
10 annual minimum VIs before integrating it over the growing season instead of using the
11 original 16-day VIs data (see in Helman et al., 2014a, 2014b and 2015). The integral over the
12 VIs during the growth season was used in the two first models against total annual ET.
13 Multiple variables regressions were applied only on NDVI and LST data or EVI and LST
14 data, but not on NDVI with EVI data because NDVI and EVI were highly correlated ($R >$
15 $0.95, p < 0.001$).

16 The original TG model is based on the observed correlations between MODIS-EVI and
17 FLUXNET GPP, which were further refined by incorporating LST data (Sims et al., 2008):

$$18 \quad GPP = a \times EVI_{scaled} \times LST_{scaled}, \quad (4)$$

19 where EVI_{scaled} is the scaled EVI set to zero at $EVI = 0.1$ (i.e., $EVI_{scaled} = EVI - 0.1$) due to
20 absence of photosynthetic activity at this value (Sims et al., 2006); a is the slope of the
21 relationship that enables parameterization of the model; and LST_{scaled} is daytime LST scaled
22 to 1 at an optimum temperature for leaf photosynthetic response around 30 °C, decreasing
23 towards 0 at lower and higher temperatures as follows (Sims et al., 2008):

$$24 \quad LST_{scaled} = \min \left[\left(\frac{LST}{30} \right); (2.5 - 0.05 \times LST) \right]. \quad (5)$$

25 Note that LST_{scaled} in Eq. (5) is negative at LST higher than 50°C. In such case, LST_{scaled} is set
26 to 0 in Eq. (4) assuming no photosynthetic activity at those high temperatures due to stomata
27 closure (Sims et al., 2008).

28 Here, we modified the TG model by using ET instead of GPP in Eq. (4):

$$29 \quad ET = a \times EVI_{scaled} \times LST_{scaled} \quad (6)$$

1 The rationale is that GPP and ET are correlated through the trade-off of carbon gain and water
2 loss through stomata opening during photosynthetic activity. We used the modified TG model
3 with EVI and NDVI alternatively in Eq. (6).

4 **3.3 Model evaluation**

5 Pearson's correlation coefficient (R) and mean absolute error (MAE) were chosen as accuracy
6 metrics to evaluate the VIs-based ET models. The best model was considered as the one with
7 the highest $|R|$ and lowest MAE or at least lower than the eddy covariance accuracy ($<30\%$).
8 If two (or more) models fulfil these requirements, the one with the best performance with
9 respect to its complexity i.e., with respect to the number of variables and operations needed,
10 was preferred. A two-tailed Student's t-test was used to examine statistical differences
11 between the models p -values.

12 **3.4 Land cover map for model implementation**

13 ET was assessed for the Eastern Mediterranean using the best models for AN and PA systems
14 separately. To produce the required land cover map, we classified pixels as AN and PA based
15 on their NDVI during the year. Low NDVI during the dry season (<0.25) implies absent or
16 dry vegetation typical for AN systems (Lu et al., 2003). Yet, some PA systems (e.g., open
17 shrublands) also have low NDVI during this period but differ from AN systems by smaller
18 NDVI change (<0.4) during the growth season (Lu et al., 2003; Roderick et al., 1999).

19 Hence, we classified pixels with minimum NDVI < 0.25 as AN only if their NDVI increased
20 by more than 0.4 during the growth season. To account for the high NDVI in agricultural
21 fields of the Nile delta, pixels with minimum NDVI smaller or equal to 0.35 were also
22 classified as AN only if their NDVI increased by more than 0.35. All remaining pixels were
23 classified as PA (Fig. S5).

24 Although this classification procedure might be coarse, we preferred it to the MODIS land
25 cover product for two reasons. First, a significant discrepancy was found between MODIS-
26 based land cover product and actual land cover type distribution in the Eastern Mediterranean
27 (Sprintsin et al., 2009a). Second, this procedure produces the required mask layer at the
28 spatial resolution of the model (250 m), while the MODIS-derived land cover product is
29 available at a coarser resolution (500 m).

30 The produced AN/PA land cover map showed the general pattern known for this region (Fig.

1 S5). Moreover, the total AN area estimated for Israel not considering the Golan Heights
2 grasslands (i.e. considering mostly Israel's croplands) was $255 \cdot 10^3$ ha. This agreed well with
3 the total cropland area reported by the Israeli Central Bureau of Statistics for the same years
4 ($220 \cdot 10^3$ ha, CBS 2014).

5

6 **4 Results and discussion**

7 **4.1 ET-VIs simple relationships in systems comprising annual and perennial** 8 **vegetation**

9 On average, the absolute correlation coefficient ($|R|$) for the ET-VIs linear regressions using
10 annual data were higher by 60% (for NDVI) and 40% (for EVI) than the $|R|$ for the 16-day
11 regressions in PA sites. Total annual ET was highly correlated with mean annual NDVI in PA
12 sites, $0.85 < R < 0.93$ (Table 3; Fig. 2). In contrast, 16-day ET averages were only poorly
13 correlated with 16-day NDVI ($0.17 < R < 0.63$). The same was for total annual ET and mean
14 annual EVI with $0.66 < R < 0.94$ compared to $0.28 < R < 0.70$ when using 16-day EVI and ET
15 data. The year-to-year changes in mean annual NDVI and EVI were significant enough to
16 detect even small interannual changes in ET of $20 - 40 \text{ mm yr}^{-1}$ (see e.g. of ES-Amo site in
17 Fig. 2).

18 LST was negatively correlated with 16-day and total annual ET in all PA FLUXNET sites.
19 This implies the role of transpiration in attenuating thermal load (Rotem-Mindali et al., 2015).
20 Mean annual LST was highly correlated with total annual ET ($|R| > 0.84$, $p < 0.05$) particularly
21 in sites with low canopy cover (IL-Yat – 30-45% and ES-LMa – 20-30%; Casals et al., 2009;
22 Sprintsin et al., 2009b). Those sites had relatively high interannual variability in LST ($2 - 3.5$
23 $^{\circ}\text{C}$; Fig. 2).

24 Correlation coefficients from the cross-site comparisons were as high as those from site-
25 specific regressions when using annual data in PA sites (Fig. 3). Correlations were equally
26 high for both, linear and exponential functions ($R = 0.94$, $p < 0.05$ for both VIs and estimating
27 functions). The linear functions were $\text{ET} = 1277 \text{ NDVI} - 189$ and $\text{ET} = 2844 \text{ EVI} - 300$ (mm
28 y^{-1}). Exponential functions were $\text{ET} = 85 e^{3.12 \text{ NDVI}}$ and $\text{ET} = 65 e^{6.31 \text{ EVI}}$ (mm y^{-1}).

29 Although a linear regression function is usually preferred to explain simple relationships
30 between two parameters, the exponential relationship is more realistic in the case of ET-VIs.

1 This is because VIs exhibit exponential relationships with LAI (Baret et al., 1989; Duchemin
2 et al., 2006), which is directly related to water consumption and ET. Also, ET is usually
3 greater than zero in places with low vegetation cover ($VIs \leq 0.1$) due to soil evaporation. The
4 mean annual NDVI and EVI explained 71 and 88% of the variability (R^2) in the total annual
5 ET using these functions. This is within the accuracy of the eddy covariance technique for
6 estimating ET (Glenn et al., 2010; Kalma et al., 2008). Cross-site correlations of annual ET
7 and LST in PA were also high with a negative relationship ($R = -0.89$, $p < 0.05$, Fig. 3).

8 The contribution of annual and perennial vegetation to VIs at the sub pixel level is most
9 difficult to distinguish in PA systems. In some cases, one of those components might have a
10 dominant contribution to VIs but insignificant for the ecosystem flux exchange (Fig. 1). This
11 is probably one of the reasons that VIs could not be used to assess ET at a seasonal timescale
12 (i.e., using 16-day data) in such systems. However, at interannual timescales (i.e., using the
13 annual mean) relationships between ET and VIs were strong and might be used to retrieve
14 total annual ET in PA systems.

15 **4.2 Comparison between empirical VIs-based ET models**

16 In AN, correlation coefficients from the cross-site regressions of ET against VIs (i.e., the
17 integrals over the growing season period) using the annual data were comparable to those
18 achieved when using the 16-day data (Table 4). The R from the linear regression using 16-day
19 was high as 0.86 for both indices ($p < 0.001$). When using the annual data, R was even higher
20 for ET-NDVI ($R = 0.88$, $p < 0.001$), but lower for ET-EVI ($R = 0.79$, $p < 0.001$). The mean
21 relative error (i.e., MAE/mean) was substantially lower for regressions using annual data (12-
22 16%) than for those using the 16-day data (32-33%, Table 5). The relatively high R for the
23 16-day ET-VIs regressions in AN supports the biomass-ET-VIs relationship in those systems
24 described elsewhere (Glenn et al., 2010).

25 Correlations did not significantly improve ($p > 0.1$) when LST was added in a multiple variable
26 regression at the AN sites (Tables 4 and 5). The R from the multiple variable regressions of
27 LST, VIs and ET was 0.87 when using 16-day data (for LST with each one of the VIs). The R
28 from the multiple variable regressions on the annual data was 0.89 and 0.79 (ET, LST and
29 NDVI or EVI, respectively with $p < 0.001$ for both).

30 In PA, correlation coefficients from the multiple variable regressions were substantially
31 higher ($p < 0.05$ using both VIs) than the obtained from simple ET-VIs regressions. R from

1 multiple variable regressions were 0.71 and 0.73 for 16-day ET against LST with NDVI or
 2 EVI, respectively compared to 0.51 and 0.61 for ET against NDVI and EVI. R from the single
 3 and multiple variable regressions were not statistically different ($p>0.1$) in PA when using
 4 annual data. The R was 0.94 and 0.96 for multiple variable models with NDVI and EVI,
 5 respectively and 0.94 for simple regression of ET against VIs (both VIs).

6 The modified TG model resulted in significantly higher R ($p<0.05$ for both indices) only for
 7 PA when using 16-day data ($R = 0.80$ and 0.78 using NDVI or EVI in Eq. (6)). However, it
 8 was still significantly lower ($p<0.05$ for both VIs) than the R obtained from simple ET–VIs
 9 regressions when using the annual data (Table 4 and Fig. S6B). In AN, the R from TG using
 10 16-day data were not significantly different than those obtained from simple ET–VIs
 11 regressions ($p>0.1$, Table 4 and Fig.S6A).

12 **4.3 PaVI-E model**

13 NDVI and EVI explained most of the interannual changes in ET in both AN and PA systems
 14 (Table 4). This means that a single ET–VIs regression function could be used to estimate total
 15 annual ET in those systems. Multiple regression and TG modified models had higher R and
 16 lower MAE in some cases (Table 5), but differences were not significant ($p>0.05$). Hence,
 17 following the performance-simplicity criterion we chose to use the simple regression
 18 functions. The functions obtained from ET-NDVI and ET-EVI regressions were averaged for
 19 PA:

$$20 \quad ET_{Annual} = \frac{85 \exp(3.1 \cdot NDVI) + 65 \exp(6.9 \cdot EVI)}{2} \quad (7)$$

21 and AN systems:

$$22 \quad ET_{Annual} = \frac{187 \exp(0.23 \cdot NDVI) + 224 \exp(0.26 \cdot EVI)}{2} \quad (8)$$

23 Where ET_{Annual} is the total annual ET in mm yr^{-1} . NDVI and EVI in Eq. (7) are the mean
 24 annual NDVI and EVI. $NDVI_{GSI}$ and EVI_{GSI} in Eq. (8) are the integrals over the NDVI and
 25 EVI during the growth season, respectively. We used exponential functions because VIs
 26 exhibit exponential relationships with LAI, which is directly related to ET and because ET is
 27 greater than zero in areas with low vegetation cover due to soil evaporation.

1 Finally, we named this model the Parameterization of Vegetation Indices for ET estimation
2 model (PaVI-E). The mean relative error of PaVI-E was 13 and 12% for AN and PA,
3 respectively. This is within the accuracy of the eddy covariance measurements that were used
4 for calibration and much lower than the reported for more complex models (Glenn et al.,
5 2010; Kalma et al., 2008). PaVI-E was used to assess total annual ET at a spatial resolution of
6 250 m for the Eastern Mediterranean (EM) after using the land cover map created for AN and
7 PA as a mask layer (Section 3.3 and Fig. S5).

8 Figure 4 shows the mean annual ET at the EM for the period of 2000-2014. The annual
9 products of PaVI-E will be soon available by request at 1 km spatial resolution for the entire
10 EM and at 250 m for Israel (<http://davidhelman.weebly.com>).

11 **4.4 Model evaluation in the Eastern Mediterranean**

12 **4.4.1 Comparison with MODIS and MSG ET models**

13 ET estimates from PaVI-E were compared with two operational remote sensing ET products
14 in 148 large basins ($>10 \text{ km}^2$). The spatial patterns of annual ET for 2011 from PaVI-E,
15 MOD16 and MSG were generally similar over the EM (Fig. 5). The three models show a
16 general west to east and south to north ET gradients along the eastern coastline, matching the
17 rainfall gradients of this region (Ziv et al., 2014). Also, all three models show higher ET
18 estimates over agricultural fields in the Nile delta compared to the surrounding desert.

19 However, some discrepancies also exist. MOD16 estimates were lower along the EM coast
20 compared to PaVI-E and MSG. ET estimates from MSG were higher along the eastern coast
21 especially to the east of the Galilee Sea (mean ET of $\sim 800 \text{ mm yr}^{-1}$). Differences between
22 models were particularly noted over the Nile delta. Annual ET for 2011 over the Nile delta
23 was on average 160 mm yr^{-1} from MSG, 530 mm yr^{-1} from MOD16, and 680 mm yr^{-1} from
24 PaVI-E. While MSG estimates seem extremely low for a such highly productive area, PaVI-E
25 and MOD16 estimates agreed well with the high ET reported from in situ measurements
26 (Elhag et al., 2011). Besides the advantage of an improved spatial resolution (250 m
27 compared to 1 km and 3.1 km of MOD16 and MSG) PaVI-E also has the ability to produce
28 spatially continuous ET compared to MSG and MODIS products (Fig. 5).

29 Comparing the three models at a basin scale resulted in good agreement between them ($R =$
30 0.77 and 0.75 for PaVI-E vs. MOD16 and MSG, respectively, $p < 0.001$ for both; Fig. 6).

1 MOD16 and MSG products had small biases with respect to PaVI-E with relative biases (i.e.,
2 bias/mean) of -5.2% and 5.2% and slopes of 0.76 and 1.17 for MOD16 and MSG ET
3 products, respectively.

4 The relatively higher (lower) MOD16 estimates in xeric (mesic) Mediterranean areas (Fig. 6)
5 was already pointed out by Trambauer et al. (2014) that compared this product with several
6 independent ET models. Furthermore, comparison of MOD16 and MSG ET products in
7 Europe showed that correlations with in situ ET (from 15-eddy covariance sites) were better
8 for MSG (Hu et al., 2015), and that MOD16 underestimate ET in Mediterranean dry regions
9 similarly to the observed in this study (Fig. 5).

10 **4.4.2 Evaluation against ET calculated from water catchment balances along** 11 **rainfall gradient**

12 ET estimates for PaVI-E were evaluated against ET calculated from six water catchments
13 along rainfall gradient in the Eastern Mediterranean (EM). PaVI-E estimates were highly
14 correlated with the ET calculated from water balances ($R = 0.92$, $p < 0.01$) at six catchments
15 along the north – south rainfall gradient in the EM (Fig. 7a). ET from MOD16 and MSG were
16 also significantly correlated with the water balances-derived ET ($p < 0.05$, Fig. S7). All three
17 models had very similar ET estimates in the mountain aquifer catchments (MA-N, MA-CS,
18 and MA-S), lower than the calculated from water balances (Fig. 7b). Still, within the accuracy
19 of the models ($\sim 12\%$) and gauging/rainfall distribution uncertainties ($\sim 10 - 15\%$, Conradt et
20 al., 2013).

21 As shown in Fig. 5, ET estimates derived from PaVI-E are significantly higher than those
22 from MOD16 and MSG in the dry areas of the EM. This is due to the exponential functions
23 used in PaVI-E (Eq. (7) and (8)). It derived a comparable ET to the calculated from the water
24 balance equation at the dry catchment of Mamashit with a slight overestimation of 15 mm
25 ($< 15\%$, Fig. 7b). MSG largely underestimated the calculated ET in Mamashit (by more than
26 85%) while MOD16 had no data for this area.

27

28 **5 Conclusions**

29 Three empirical VIs-based ET models using only eddy covariance ET and MODIS vegetation
30 indices and land surface temperature data for Mediterranean vegetation systems were tested.
31 Vegetation systems comprising mostly annual vegetation (i.e., grasslands and croplands) had

1 strong ET-VIs relationships with intra-annual (16-day ET averages) and interannual (total
2 annual ET) ET estimates. The mean relative error was larger for intra-annual relationships
3 compared to interannual relationships (32% compared to 12%). In systems with annual and
4 perennial vegetation (i.e., forests, woodlands, savannah and shrublands) ET-VIs relationships
5 were strong only at interannual timescales (i.e., using annual data). Intra-annual relationships
6 were poor probably due to the mixed VI signal contributed by annual and perennial vegetation
7 that constitute different vertical layers in those systems (Helman et al., 2015). While annual
8 vegetation (mostly herbaceous vegetation in the understory) is the main contributor to the
9 intra-annual VI change, it constitutes only a minor contributor to the total ecosystem ET in
10 complex Mediterranean systems. Multiple variable regression and modified TG models using
11 VIs and LST were not significantly better than the simple ET-VIs model for both PA and AN
12 vegetation systems ($p>0.1$).

13 The empirical ET-VIs model, named here the parameterized vegetation index for ET
14 estimates model (PaVI-E), had comparable estimates to MODIS and MSG ET models in the
15 Eastern Mediterranean. PaVI-E also agreed well with ET calculated using the water balance
16 equation at six catchments along the south-north EM rainfall gradient. PaVI-E is the first ET
17 model with such high-resolution (250 m) for this region. Its advantage is in its simplicity and
18 spatial resolution compared to the coarser resolutions of MODIS and MSG ET products (1
19 and 3.1 km, respectively). We are confident that using PaVI-E will enhance the hydrological
20 study in this region where ET plays a major role in the hydrological cycle.

21

22 **Acknowledgements**

23 This research was supported by the Hydrological Service of Israel (HSI), Water Authority
24 (Grant No. 4500962964). David Helman greatly acknowledges personal grants provided by
25 the JNF-Rieger Foundation, USA and the HSI. Authors thank two anonymous referees and
26 Prof. Janne Rinne for their comments and suggestions that improved the previous version of
27 this manuscript. This study used eddy covariance data acquired by the FLUXNET community
28 and in particular by the following networks: AmeriFlux (U.S. Department of Energy,
29 Biological and Environmental Research, Terrestrial Carbon Program), CarboItaly and
30 CarboEuropeIP. MODIS subsets and tiles land products were acquired from the Oak Ridge
31 National Laboratory Distributed Active Archive Centre (ORNL DAAC) and the U.S.
32 Geological Survey (USGS).

1 References

- 2 Anderson, M. C., Norman, J. M., Kustas, W. P., Houborg, R., Starks, P. J. and Agam, N.: A
3 thermal-based remote sensing technique for routine mapping of land-surface carbon, water
4 and energy fluxes from field to regional scales, *Remote Sensing of Environment*, 112(12),
5 4227–4241, doi:10.1016/j.rse.2008.07.009, 2008.
- 6 Baldocchi, D. D., Xu, L. and Kiang, N.: How plant functional-type, weather, seasonal
7 drought, and soil physical properties alter water and energy fluxes of an oak–grass savanna
8 and an annual grassland, *Agricultural and Forest Meteorology*, 123(1–2), 13–39,
9 doi:10.1016/j.agrformet.2003.11.006, 2004.
- 10 Baret, F., Guyot, G. and Major, D. J.: Crop biomass evaluation using radiometric
11 measurements, *Photogrammetria*, 43(5), 241–256, doi:10.1016/0031-8663(89)90001-X, 1989.
- 12 Casals, P., Gimeno, C., Carrara, A., Lopez-Sangil, L. and Sanz, M.: Soil CO₂ efflux and
13 extractable organic carbon fractions under simulated precipitation events in a Mediterranean
14 Dehesa, *Soil Biology and Biochemistry*, 41(9), 1915–1922,
15 doi:10.1016/j.soilbio.2009.06.015, 2009.
- 16 Chamizo, S., Cantón, Y., Miralles, I. and Domingo, F.: Biological soil crust development
17 affects physicochemical characteristics of soil surface in semiarid ecosystems, *Soil Biology
18 and Biochemistry*, 49(0), 96–105, doi:10.1016/j.soilbio.2012.02.017, 2012.
- 19 Chen, X., Su, Z., Ma, Y., Liu, S., Yu, Q. and Xu, Z.: Development of a 10-year (2001–2010)
20 0.1° data set of land-surface energy balance for mainland China, *Atmos. Chem. Phys.*, 14(23),
21 13097–13117, doi:10.5194/acp-14-13097-2014, 2014.
- 22 Colaizzi, P. D., Kustas, W. P., Anderson, M. C., Agam, N., Tolck, J. A., Evett, S. R., Howell,
23 T. A., Gowda, P. H. and O’Shaughnessy, S. A.: Two-source energy balance model estimates
24 of evapotranspiration using component and composite surface temperatures, *Advances in
25 Water Resources*, 50(0), 134–151, doi:10.1016/j.advwatres.2012.06.004, 2012.
- 26 Conradt, T., Wechsung, F. and Bronstert, A.: Three perceptions of the evapotranspiration
27 landscape: comparing spatial patterns from a distributed hydrological model, remotely sensed
28 surface temperatures, and sub-basin water balances, *Hydrology and Earth System Sciences*,
29 17(7), 2947–2966, doi:10.5194/hess-17-2947-2013, 2013.
- 30 Craine, J. M., Nippert, J. B., Elmore, A. J., Skibbe, A. M., Hutchinson, S. L. and Brunsell, N.
31 A.: Timing of climate variability and grassland productivity, *Proceedings of the National
32 Academy of Sciences*, 109(9), 3401–3405, 2012.
- 33 Duchemin, B., Hadria, R., Erraki, S., Boulet, G., Maisongrande, P., Chehbouni, A., Escadafal,
34 R., Ezzahar, J., Hoedjes, J. C. B., Kharrou, M. H., Khabba, S., Mougenot, B., Olioso, A.,
35 Rodriguez, J.-C. and Simonneaux, V.: Monitoring wheat phenology and irrigation in Central
36 Morocco: On the use of relationships between evapotranspiration, crops coefficients, leaf area
37 index and remotely-sensed vegetation indices, *Agricultural Water Management*, 79(1), 1–27,
38 doi:10.1016/j.agwat.2005.02.013, 2006.

- 1 Elhag, M., Psilovikos, A., Manakos, I. and Perakis, K.: Application of the SEBS water
2 balance model in estimating daily evapotranspiration and evaporative fraction from remote
3 sensing data over the Nile delta, *Water Resour Manage*, 25(11), 2731–2742,
4 doi:10.1007/s11269-011-9835-9, 2011.
- 5 Glenn, E., Nagler, P. and Huete, A.: Vegetation index methods for estimating
6 evapotranspiration by remote sensing, *Surv Geophys*, 31(6), 531–555, doi:10.1007/s10712-
7 010-9102-2, 2010.
- 8 Glenn, E. P., Neale, C. M. U., Hunsaker, D. J. and Nagler, P. L.: Vegetation index-based crop
9 coefficients to estimate evapotranspiration by remote sensing in agricultural and natural
10 ecosystems, *Hydrol. Process.*, 25(26), 4050–4062, doi:10.1002/hyp.8392, 2011.
- 11 Helman, D., Mussery, A., Lensky, I. M. and Leu, S.: Detecting changes in biomass
12 productivity in a different land management regimes in drylands using satellite-derived
13 vegetation index, *Soil Use Manage*, 30(1), 32–39, doi:10.1111/sum.12099, 2014a.
- 14 Helman, D., Lensky, I. M., Mussery, A. and Leu, S.: Rehabilitating degraded drylands by
15 creating woodland islets: Assessing long-term effects on aboveground productivity and soil
16 fertility, *Agricultural and Forest Meteorology*, 195–196(0), 52–60,
17 doi:10.1016/j.agrformet.2014.05.003, 2014b.
- 18 Helman, D., Lensky, I. M., Tessler, N. and Osem, Y.: A phenology-based method for
19 monitoring woody and herbaceous vegetation in Mediterranean forests from NDVI time
20 series, *Remote Sensing*, 7, 12314–12335, doi:10.3390/rs70912314, 2015.
- 21 Hollinger, S. E., Bernacchi, C. J. and Meyers, T. P.: Carbon budget of mature no-till
22 ecosystem in North Central Region of the United States, *Agricultural and Forest Meteorology*,
23 130(1–2), 59–69, doi:10.1016/j.agrformet.2005.01.005, 2005.
- 24 Huete, A., Didan, K., Miura, T., Rodriguez, E. P., Gao, X. and Ferreira, L. G.: Overview of
25 the radiometric and biophysical performance of the MODIS vegetation indices, *Remote*
26 *sensing of environment*, 83(1), 195–213, 2002.
- 27 Hu, G., Jia, L. and Menenti, M.: Comparison of MOD16 and LSA-SAF MSG
28 evapotranspiration products over Europe for 2011, *Remote Sensing of Environment*, 156(0),
29 510–526, doi:10.1016/j.rse.2014.10.017, 2015.
- 30 Jung, M., Reichstein, M. and Bondeau, A.: Towards global empirical upscaling of FLUXNET
31 eddy covariance observations: validation of a model tree ensemble approach using a
32 biosphere model, *Biogeosciences*, 6(10), 2001–2013, doi:10.5194/bg-6-2001-2009, 2009.
- 33 Jung, M., Reichstein, M., Ciais, P., Seneviratne, S. I., Sheffield, J., Goulden, M. L., Bonan,
34 G., Cescatti, A., Chen, J., de Jeu, R., Dolman, A. J., Eugster, W., Gerten, D., Gianelle, D.,
35 Gobron, N., Heinke, J., Kimball, J., Law, B. E., Montagnani, L., Mu, Q., Mueller, B., Oleson,
36 K., Papale, D., Richardson, A. D., Rouspard, O., Running, S., Tomelleri, E., Viovy, N.,
37 Weber, U., Williams, C., Wood, E., Zaehle, S. and Zhang, K.: Recent decline in the global
38 land evapotranspiration trend due to limited moisture supply, *Nature*, 467(7318), 951–954,
39 doi:10.1038/nature09396, 2010.

- 1 Kalma, J., McVicar, T. and McCabe, M.: Estimating land surface evaporation: A review of
2 methods using remotely sensed surface temperature data, *Surv Geophys*, 29(4-5), 421–469,
3 doi:10.1007/s10712-008-9037-z, 2008.
- 4 Karnieli, A.: Natural vegetation phenology assessment by ground spectral measurements in
5 two semi-arid environments, *Int J Biometeorol*, 47(4), 179–187, doi:10.1007/s00484-003-
6 0169-z, 2003.
- 7 Kutsch, W. L., Aubinet, M., Buchmann, N., Smith, P., Osborne, B., Eugster, W., Wattenbach,
8 M., Schruppf, M., Schulze, E. D., Tomelleri, E., Ceschia, E., Bernhofer, C., Béziat, P.,
9 Carrara, A., Di Tommasi, P., Grünwald, T., Jones, M., Magliulo, V., Marloie, O., Moureaux,
10 C., Olioso, A., Sanz, M. J., Saunders, M., Søgaard, H. and Ziegler, W.: The net biome
11 production of full crop rotations in Europe, *Agriculture, Ecosystems & Environment*, 139(3),
12 336–345, doi:10.1016/j.agee.2010.07.016, 2010.
- 13 Lu, H., Raupach, M. R., McVicar, T. R. and Barrett, D. J.: Decomposition of vegetation cover
14 into woody and herbaceous components using AVHRR NDVI time series, *Remote Sensing of
15 Environment*, 86(1), 1–18, doi:10.1016/S0034-4257(03)00054-3, 2003.
- 16 Maeda, E. E., Wiberg, D. A. and Pellikka, P. K. E.: Estimating reference evapotranspiration
17 using remote sensing and empirical models in a region with limited ground data availability in
18 Kenya, *Applied Geography*, 31(1), 251–258, doi:10.1016/j.apgeog.2010.05.011, 2011.
- 19 Maselli, F., Papale, D., Chiesi, M., Matteucci, G., Angeli, L., Raschi, A. and Seufert, G.:
20 Operational monitoring of daily evapotranspiration by the combination of MODIS NDVI and
21 ground meteorological data: Application and evaluation in Central Italy, *Remote Sensing of
22 Environment*, 152(0), 279–290, doi:10.1016/j.rse.2014.06.021, 2014.
- 23 Maseyk, K. S., Lin, T., Rotenberg, E., Grünzweig, J. M., Schwartz, A. and Yakir, D.:
24 Physiology–phenology interactions in a productive semi-arid pine forest, *New Phytologist*,
25 178(3), 603–616, 2008.
- 26 Ma, Y., Zhu, Z., Zhong, L., Wang, B., Han, C., Wang, Z., Wang, Y., Lu, L., Amatya, P. M.,
27 Ma, W. and Hu, Z.: Combining MODIS, AVHRR and in situ data for evapotranspiration
28 estimation over heterogeneous landscape of the Tibetan Plateau, *Atmos. Chem. Phys.*, 14(3),
29 1507–1515, doi:10.5194/acp-14-1507-2014, 2014.
- 30 Moffat, A. M., Papale, D., Reichstein, M., Hollinger, D. Y., Richardson, A. D., Barr, A. G.,
31 Beckstein, C., Braswell, B. H., Churkina, G. and Desai, A. R.: Comprehensive comparison of
32 gap-filling techniques for eddy covariance net carbon fluxes, *Agricultural and Forest
33 Meteorology*, 147(3), 209–232, 2007.
- 34 Nagler, P. L., Brown, T., Hultine, K. R., van Riper III, C., Bean, D. W., Dennison, P. E.,
35 Murray, R. S. and Glenn, E. P.: Regional scale impacts of Tamarix leaf beetles (*Diorhabda
36 carinulata*) on the water availability of western U.S. rivers as determined by multi-scale
37 remote sensing methods, *Remote Sensing of Environment*, 118(0), 227–240,
38 doi:10.1016/j.rse.2011.11.011, 2012.
- 39 Oki, T. and Kanae, S.: Global Hydrological Cycles and World Water Resources, *Science*,
40 313(5790), 1068–1072, 2006.

- 1 Reichstein, M., Falge, E., Baldocchi, D., Papale, D., Aubinet, M., Berbigier, P., Bernhofer, C.,
2 Buchmann, N., Gilmanov, T., Granier, A., Grünwald, T., Havránková, K., Ilvesniemi, H.,
3 Janous, D., Knohl, A., Laurila, T., Lohila, A., Loustau, D., Matteucci, G., Meyers, T.,
4 Miglietta, F., Ourcival, J.-M., Pumpanen, J., Rambal, S., Rotenberg, E., Sanz, M., Tenhunen,
5 J., Seufert, G., Vaccari, F., Vesala, T., Yakir, D. and Valentini, R.: On the separation of net
6 ecosystem exchange into assimilation and ecosystem respiration: review and improved
7 algorithm, *Global Change Biology*, 11(9), 1424–1439, doi:10.1111/j.1365-
8 2486.2005.001002.x, 2005.
- 9 Reichstein, M., Ciais, P., Papale, D., Valentini, R., Running, S., Viovy, N., Cramer, W.,
10 Granier, A., Ogee, J., Allard, V., Aubinet, M., Bernhofer, C., Buchmann, N., Carrara, A.,
11 Grünwald, T., Heimann, M., Heinesch, B., Knohl, A., Kutsch, W., Loustau, D., Manca, G.,
12 Matteucci, G., Miglietta, F., Ourcival, J. M., Pilegaard, K., Pumpanen, J., Rambal, S.,
13 Schaphoff, S., Seufert, G., Soussana, J.-F., Sanz, M.-J., Vesala, T. and Zhao, M.: Reduction of
14 ecosystem productivity and respiration during the European summer 2003 climate anomaly: a
15 joint flux tower, remote sensing and modelling analysis, *Global Change Biology*, 13(3), 634–
16 651, doi:10.1111/j.1365-2486.2006.01224.x, 2007.
- 17 Roderick, M. L., Noble, I. R. and Cridland, S. W.: Estimating woody and herbaceous
18 vegetation cover from time series satellite observations, *Global Ecology and Biogeography*,
19 8(6), 501–508, doi:10.1046/j.1365-2699.1999.00153.x, 1999.
- 20 Rotem-Mindali, O., Michael, Y., Helman, D. and Lensky, I. M.: The role of local land-use on
21 the urban heat island effect of Tel Aviv as assessed from satellite remote sensing, *Applied*
22 *Geography*, 56(0), 145–153, doi:10.1016/j.apgeog.2014.11.023, 2015.
- 23 Rouse, J. W., Haas, R. H. and Schell, J. A.: Monitoring the vernal advancement and
24 retrogradation (greenwave effect) of natural vegetation, Texas A and M University, College
25 Station., 1974.
- 26 Scott, R. L., Hamerlynck, E. P., Jenerette, G. D., Moran, M. S. and Barron-Gafford, G. A.:
27 Carbon dioxide exchange in a semidesert grassland through drought-induced vegetation
28 change, *J. Geophys. Res.*, 115(G3), G03026, doi:10.1029/2010JG001348, 2010.
- 29 Senay, G. B., Leake, S., Nagler, P. L., Artan, G., Dickinson, J., Cordova, J. T. and Glenn, E.
30 P.: Estimating basin scale evapotranspiration (ET) by water balance and remote sensing
31 methods, *Hydrol. Process.*, 25(26), 4037–4049, doi:10.1002/hyp.8379, 2011.
- 32 Shi, Q. and Liang, S.: Surface-sensible and latent heat fluxes over the Tibetan Plateau from
33 ground measurements, reanalysis, and satellite data, *Atmos. Chem. Phys.*, 14(11), 5659–5677,
34 doi:10.5194/acp-14-5659-2014, 2014.
- 35 Sims, D. A., Rahman, A. F., Cordova, V. D., El-Masri, B. Z., Baldocchi, D. D., Flanagan, L.
36 B., Goldstein, A. H., Hollinger, D. Y., Misson, L., Monson, R. K., Oechel, W. C., Schmid, H.
37 P., Wofsy, S. C. and Xu, L.: On the use of MODIS EVI to assess gross primary productivity
38 of North American ecosystems, *J. Geophys. Res.*, 111(G4), G04015,
39 doi:10.1029/2006JG000162, 2006.
- 40 Sims, D. A., Rahman, A. F., Cordova, V. D., El-Masri, B. Z., Baldocchi, D. D., Bolstad, P.
41 V., Flanagan, L. B., Goldstein, A. H., Hollinger, D. Y., Misson, L., Monson, R. K., Oechel,

- 1 W. C., Schmid, H. P., Wofsy, S. C. and Xu, L.: A new model of gross primary productivity
2 for North American ecosystems based solely on the enhanced vegetation index and land
3 surface temperature from MODIS, *Remote Sensing of Environment*, 112(4), 1633–1646,
4 doi:10.1016/j.rse.2007.08.004, 2008.
- 5 Skiba, U., Drewer, J., Tang, Y. S., van Dijk, N., Helfter, C., Nemitz, E., Famulari, D., Cape, J.
6 N., Jones, S. K., Twigg, M., Pihlatie, M., Vesala, T., Larsen, K. S., Carter, M. S., Ambus, P.,
7 Ibrom, A., Beier, C., Hensen, A., Frumau, A., Erisman, J. W., Brüggemann, N., Gasche, R.,
8 Butterbach-Bahl, K., Neftel, A., Spirig, C., Horvath, L., Freibauer, A., Cellier, P., Laville, P.,
9 Loubet, B., Magliulo, E., Bertolini, T., Seufert, G., Andersson, M., Manca, G., Laurila, T.,
10 Aurela, M., Lohila, A., Zechmeister-Boltenstern, S., Kitzler, B., Schaufler, G., Siemens, J.,
11 Kindler, R., Flechard, C. and Sutton, M. A.: Biosphere–atmosphere exchange of reactive
12 nitrogen and greenhouse gases at the NitroEurope core flux measurement sites: Measurement
13 strategy and first data sets, *Agriculture, Ecosystems & Environment*, 133(3–4), 139–149,
14 doi:10.1016/j.agee.2009.05.018, 2009.
- 15 Sprintsin, M., Karnieli, A., Berliner, P., Rotenberg, E., Yakir, D. and Cohen, S.: Evaluating
16 the performance of the MODIS Leaf Area Index (LAI) product over a Mediterranean dryland
17 planted forest, *International Journal of Remote Sensing*, 30(19), 5061–5069,
18 doi:10.1080/01431160903032885, 2009a.
- 19 Sprintsin, M., Karnieli, A., Sprintsin, S., Cohen, S. and Berliner, P.: Relationships between
20 stand density and canopy structure in a dryland forest as estimated by ground-based
21 measurements and multi-spectral spaceborne images, *Journal of Arid Environments*, 73(10),
22 955–962, doi:10.1016/j.jaridenv.2009.04.011, 2009b.
- 23 Suyker, A. E. and Verma, S. B.: Interannual water vapor and energy exchange in an irrigated
24 maize-based agroecosystem, *Agricultural and Forest Meteorology*, 148(3), 417–427,
25 doi:10.1016/j.agrformet.2007.10.005, 2008.
- 26 Tillman, F. D., Callegary, J. B., Nagler, P. L. and Glenn, E. P.: A simple method for
27 estimating basin-scale groundwater discharge by vegetation in the basin and range province of
28 Arizona using remote sensing information and geographic information systems, *Journal of*
29 *Arid Environments*, 82(0), 44–52, doi:10.1016/j.jaridenv.2012.02.010, 2012.
- 30 Trambauer, P., Dutra, E., Maskey, S., Werner, M., Pappenberger, F., van Beek, L. P. H. and
31 Uhlenbrook, S.: Comparison of different evaporation estimates over the African continent,
32 *Hydrology and Earth System Sciences*, 18(1), 193–212, doi:10.5194/hess-18-193-2014, 2014.
- 33 Tsarouchi, G. M., Buytaert, W. and Mijic, A.: Coupling a land-surface model with a crop
34 growth model to improve ET flux estimations in the Upper Ganges basin, India, *Hydrol. Earth*
35 *Syst. Sci.*, 18(10), 4223–4238, doi:10.5194/hess-18-4223-2014, 2014.
- 36 Wilson, T. B. and Meyers, T. P.: Determining vegetation indices from solar and
37 photosynthetically active radiation fluxes, *Agricultural and Forest Meteorology*, 144(3–4),
38 160–179, doi:10.1016/j.agrformet.2007.04.001, 2007.
- 39 Zemp, D. C., Schleussner, C.-F., Barbosa, H. M. J., van der Ent, R. J., Donges, J. F., Heinke,
40 J., Sampaio, G. and Rammig, A.: On the importance of cascading moisture recycling in South
41 America, *Atmos. Chem. Phys.*, 14(23), 13337–13359, doi:10.5194/acp-14-13337-2014, 2014.

1 Ziv, B., Saaroni, H., Pargament, R., Harpaz, T. and Alpert, P.: Trends in rainfall regime over
2 Israel, 1975–2010, and their relationship to large-scale variability, *Reg Environ Change*,
3 14(5), 1751–1764, doi:10.1007/s10113-013-0414-x, 2014.

4

1 Table 1. Description of the 16 selected FLUXNET sites. Horizontal line divides between the
 2 six FLUXNET sites in PA systems (Top) and the nine FLUXNET sites in AN systems
 3 (Bottom). Plant functional types (PFT) include CSH: closed shrublands, WDL: woodland,
 4 SAV: savannah, ENF: evergreen needle-leaved forest, WSA: woody savannah, CRO:
 5 croplands, and GRA: grasslands. Mean annual precipitation (P) is in mm yr^{-1} for the years in
 6 which ET data was used (Period).

Site ID	Lat	Lon	PFT	Main species	P	Period	Reference
ES-Amo	36.83	-2.25	OSH	Dwarf shrubs	200	2009–11	Chamizo et al. (2012)
IL-Yat	31.35	35.05	WDL	<i>Pinus halepensis</i>	300	2003–09	Maseyk et al. (2008)
ES-LMa	39.94	-5.77	SAV	<i>Quercus ilex</i>	660	2004–09	Casals et al. (2009)
ES-ES	39.35	-0.32	ENF	<i>Pinus halepensis</i>	580	2001–06	Reichstein et al. (2007)
FR-Lbr	44.72	-0.77	WSA	<i>Pinus pinaster</i>	825	2004–08	Reichstein et al. (2007)
US-Blo	38.90	-120.63	ENF	<i>Pinus ponderosa</i>	1350	2001–06	Sims et al. (2006)
ES-ES2	39.28	-0.32	CRO	Rice	620	2005–08	Kutsch et al. (2010)
IT-Cas	45.07	8.72	CRO	Rice	960	2007–10	Skiba et al. (2009)
US-Bo1	40.01	-88.29	CRO	Corn–soybeans	795	2001–06	Hollinger et al. (2005)
US-Ne1	41.17	-96.48	CRO	Maize	590	2002–04	Suyker and Verma (2008)
US-Ne2	41.16	-96.47	CRO	Maize–soybean	590	2002–04	Suyker and Verma (2008)
US-Ne3	41.18	-96.44	CRO	Maize–soybean	590	2002–05	Suyker and Verma (2008)
US-Var	38.41	-120.95	GRA	C3 grass & herbs	465	2003–09	Baldocchi et al. (2004)
US-Kon	39.08	-96.56	GRA	C4 grasses	660	2007–12	Craine et al. (2012)
US-Wkg	31.74	-109.94	GRA	C4 grasses	190	2005–07	Scott et al. (2010)
US-Goo	34.25	-89.87	GRA	C4 grasses	1300	2003–06	Wilson and Meyers (2007)

1 Table 2. Water balances from six catchments along the north to south rainfall gradient in the
 2 Eastern Mediterranean (Fig. S2). Catchments area is in 10^3 ha. Precipitation (P), discharge
 3 (Q) and calculated ET as $P - Q$, are all in mm yr^{-1} . Fluxes were averaged over the years 2000
 4 – 2013. MA-N, MA-CS and MA-S stand for the northern, central-southern and southern parts
 5 of the Mountain Aquifer of Israel, respectively, as defined by the Hydrological Service of
 6 Israel (HSI).

Name	Area	P	Q	ET
Kziv	13	799	284	515
HaShofet	1.2	654	183	471
MA-N	59	615	193	422
MA-CS	93	592	202	390
MA-S	28	619	257	362
Mamashit	6	130	28	102

7

1 Table 3. Correlation coefficients (R) from the linear regression between eddy covariance ET
 2 and MODIS NDVI, EVI and LST using 16-day and annual data at six FLUXNET sites in PA
 3 systems (perennials and annuals vegetation systems, i.e. forests, woodlands, savannah and
 4 shrublands). Statistically significant correlations at $p < 0.05$ were indicated by * while **
 5 indicates $p = 0.06$ and *** $p = 0.07$.

Site ID	NDVI		EVI		LST	
	16-day	Annual	16-day	Annual	16-day	Annual
ES-Amo	0.63*	0.89	0.62*	0.71	-0.51*	-0.33
IL-Yat	0.62*	0.88*	0.70*	0.89*	-0.36*	-0.84*
ES-LMa	0.17**	0.93*	0.28*	0.80**	-0.22*	-0.93*
ES-ES	0.41*	0.91*	0.30*	0.94*	-0.62*	-0.32
FR-Lbr	0.36*	0.85***	0.68*	0.93*	-0.65*	-0.63
US-Blo	0.17**	0.92*	0.46*	0.66	-0.87*	-0.59

6

1 Table 4. Correlations coefficients (R) of three empirical VIs-based ET models using MODIS-
 2 derived NDVI, EVI and LST. Results are for models using 16-day/annual data in AN (annual
 3 vegetation systems i.e., croplands and grasslands), and PA (perennials and annuals vegetation
 4 systems i.e., forests, savannah and shrublands) systems. All R were significant at $p < 0.05$
 5 except for the 16-day ET-LST simple regression in PA. Mean annual NDVI and EVI were
 6 regressed against annual ET using linear and exponential functions.

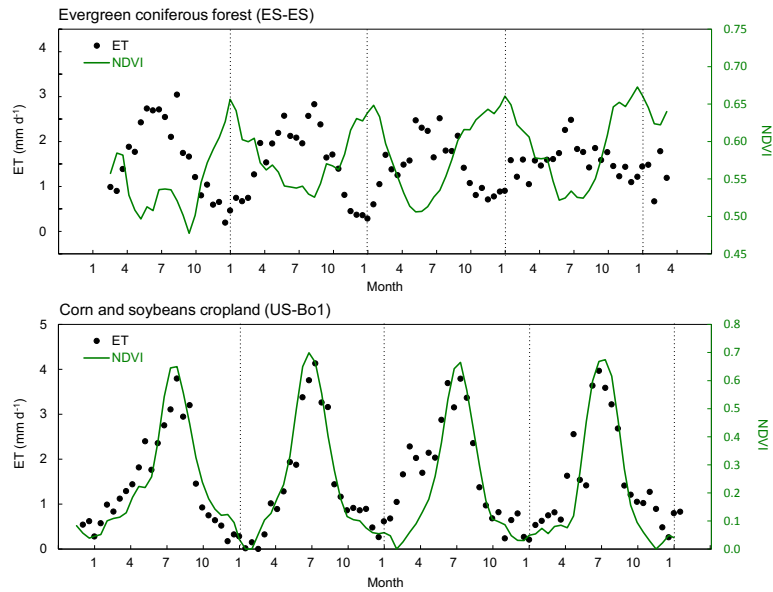
Model type	Variables used	AN		PA	
		16-day	Annual	16-day	Annual
Simple regression	NDVI (linear)	0.86	0.88	0.51	0.94
	NDVI (expo)	–	0.87	–	0.94
	EVI (linear)	0.86	0.79	0.61	0.95
	EVI (expo)	–	0.82	–	0.94
	LST	-0.42	-0.64	0.00 ^{ns}	-0.89
Multiple regression	NDVI, LST	0.87	0.89	0.71	0.94
	EVI, LST	0.87	0.79	0.73	0.96
Modified TG	NDVI, LST _{scaled}	0.87	–	0.78	–
	EVI, LST _{scaled}	0.87	–	0.80	–

7

1 Table 5. The mean absolute error (MAE) for Table 4. The 16-day MAE is in mm d^{-1} , while
 2 annual MAE is in mm y^{-1} . In parenthesis is the mean relative error (MAE/mean) in %.

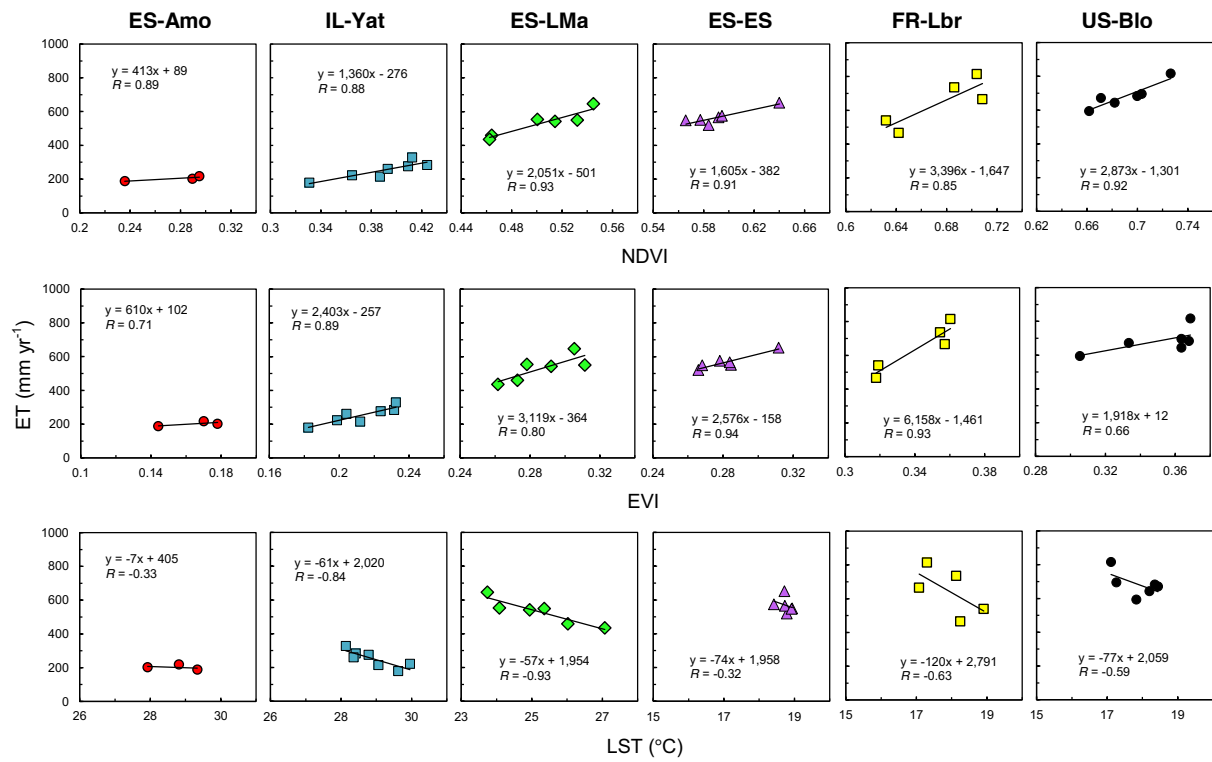
Model type	Variables used	AN		PA	
		16-day	Annual	16-day	Annual
Simple regression	NDVI (linear)	0.51(32)	66(12)	0.65(47)	52(11)
	NDVI (expo)	–	83(15)	–	58(12)
	EVI (linear)	0.52(33)	79(14)	0.59(43)	53(11)
	EVI (expo)	–	90(16)	–	63(13)
	LST	0.94(60)	119(21)	0.78(57) ^{ns}	74(15)
Multiple regression	NDVI, LST	0.51(32)	63(11)	0.57(41)	52(11)
	EVI, LST	0.51(33)	79(14)	0.54(40)	49(10)
Modified TG	NDVI, LST _{scaled}	0.48(30)	–	0.47(34)	–
	EVI, LST _{scaled}	0.50(32)	–	0.45(33)	–

3



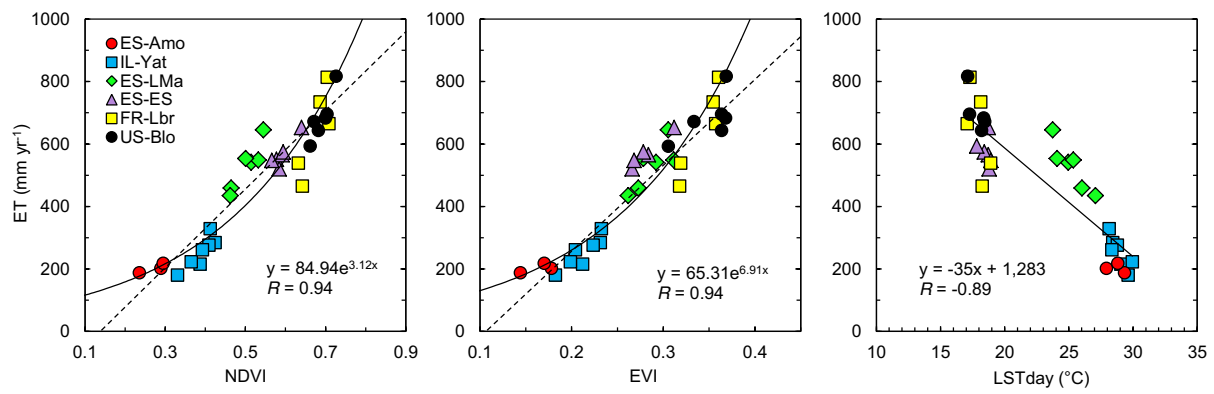
1
 2 Figure 1. Sixteen-day eddy covariance ET averages and MODIS-derived NDVI at two
 3 vegetation systems: (Top) PA, i.e. comprising perennial and annual vegetation (evergreen
 4 coniferous forest), and (Bottom) AN, i.e. annual vegetation alone (corn and soybean
 5 cropland). Note: In the cropland site (Bottom) is the NDVI during the growing season after
 6 the annual minimum was subtracted.

7



1
2
3
4
5

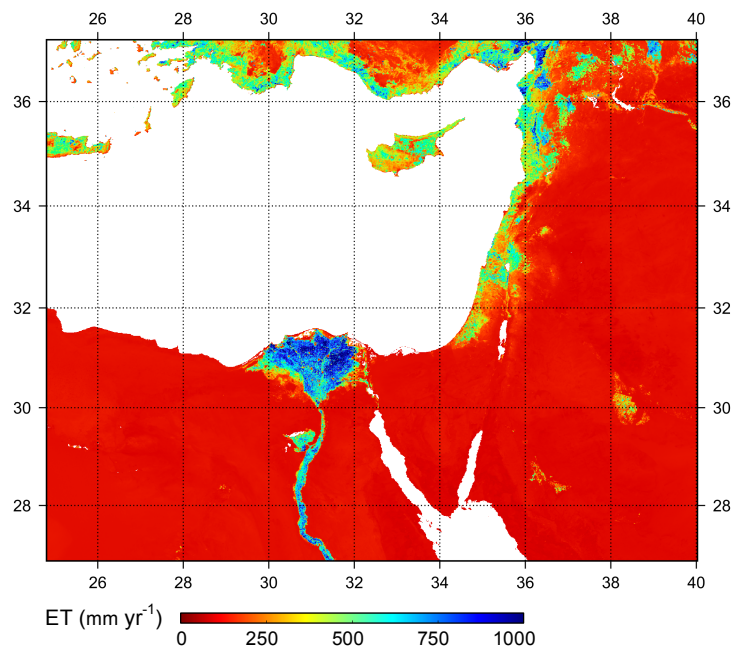
Figure 2. Relationships between annual ET (mm yr^{-1}) from eddy covariance towers and mean annual MODIS-derived NDVI, EVI and LST ($^{\circ}\text{C}$) in PA sites (perennials and annuals vegetation systems, i.e. forests, woodlands, savannah and shrublands).



1

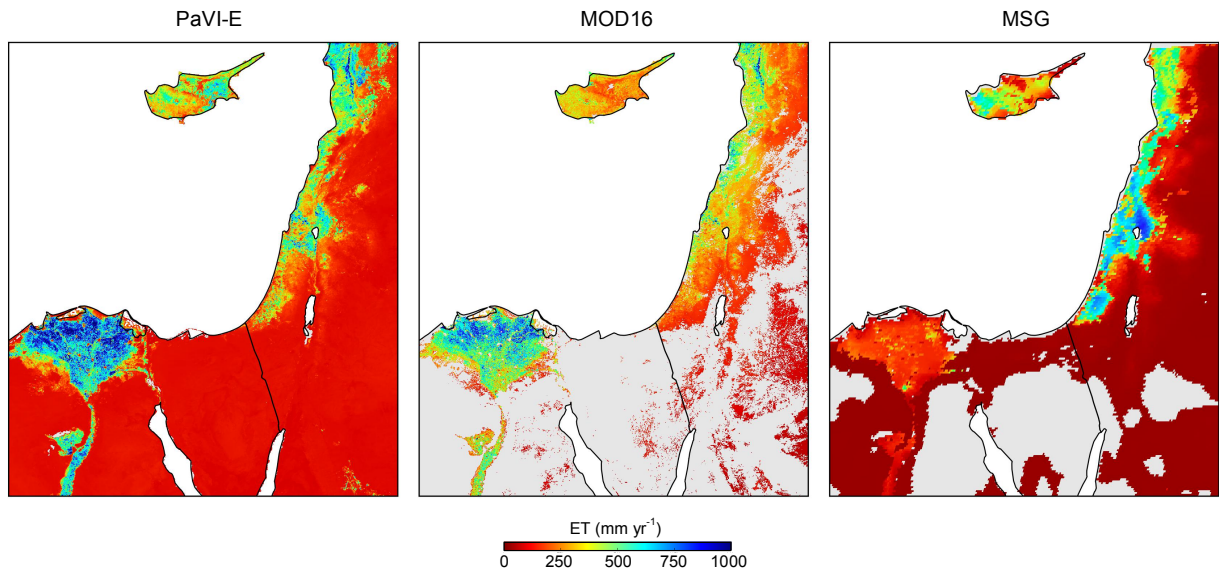
2 Figure 3. Same as Fig. 2 but for all PA sites together. The linear (dashed line) and exponential
 3 (solid line) functions are presented for the ET-VIs relationships and the R is for the
 4 exponential function.

5



1

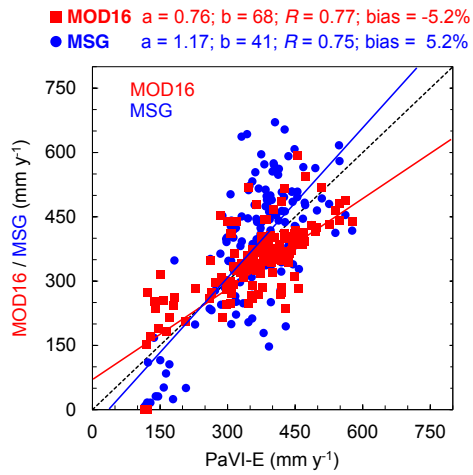
2 Figure 4. Mean annual ET (2000–2014) from PaVI-E for the Eastern Mediterranean.



1

2 Figure 5. Total annual ET for the Eastern Mediterranean from PaVI-E, MODIS (MOD16) and
 3 MSG (LSA-SAF MSG ETa) for 2011. Grey colour in MOD16 and MSG indicates missing
 4 data.

5

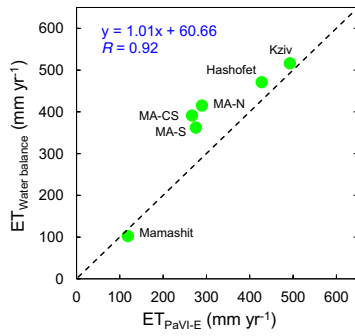


1

2 Figure 6. Total annual ET at 148 Eastern Mediterranean basins (Fig. S1) from MODIS
 3 (MOD16) and MSG (LSA-SAF MSG ETa) vs. PaVI-E. The slope (a), intersection (b),
 4 Pearson's (R) and relative bias (bias/mean) are also presented for each one of the linear
 5 regressions. Dashed line indicates the 1:1 ratio.

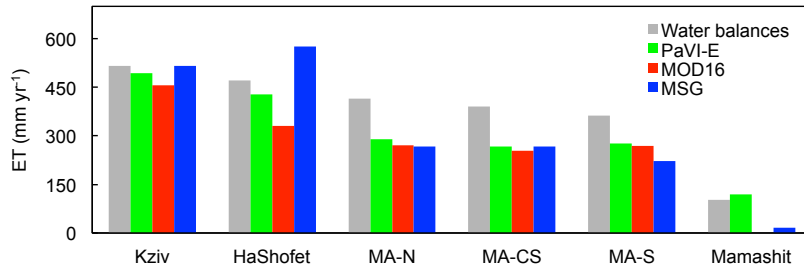
6

a



1

b



2

3

4 Figure 7. (a) Scatter plot of the mean annual ET (2000-2013) retrieved from PaVI-E and
5 calculated using the water balance equation at six catchments along the EM north – south
6 rainfall gradient (Fig. S2). (b) Comparison between mean annual ET estimates from PaVI-E,
7 MOD16, MSG and the water balances in those six water catchments. MA-N, MA-CS and
8 MA-S stand for the northern, central-southern, and southern parts of the Mountain Aquifer of
9 Israel, respectively.